Photoacoustic Imaging Guided Near-Infrared Photothermal Therapy Using Highly Water-Dispersible Single-Walled Carbon Nanohorns as Theranostic Agents

Daiqin Chen, Chao Wang, Xin Nie, Shumu Li, Ruimin Li, Mirong Guan, Zhuang Liu, Chunying Chen, Chunru Wang, Chunying Shu, and Lijun Wan**

The poly(maleic anhydride-alt-1-octadecene-poly(ethylene glycol)) (C_{18}PMH-PEG) modified single-walled carbon nanohorns (SWNHs) are designed with high stability and biocompatibility. The as-prepared SWNHs/C_{18}PMH-PEG not only can serve as an excellent photothermal agent but also can be used as a promising photoacoustic imaging (PAI) agent both in vitro and in vivo due to its strong absorption in the near infrared (NIR) region. The PAI result reveals that the SWNHs/C_{18}PMH-PEG possesses ultra long blood circulation time and can significantly be accumulated at the tumor site through the enhanced penetration and retention (EPR) effect. The maximum accumulation of SWNHs/C_{18}PMH-PEG at tumor site could be achieved at the time point of 24 h after intravenous injection, which is considered to be the optimal time for the 808 nm laser treatment. The subsequent photothermal ablation of tumors can be achieved without triggering any side effects. Therefore, a PAI guided PTT platform based on SWNHs is proposed and highlights the potential theranostic application for biomedical uses.

1. Introduction

Photothermal therapy (PTT) has attracted much attention due to its highly specific selectivity to targeting sites and non-invasiveness to normal tissues.[1–3] Up to date, large quantities of photothermal agents have been reported, such as gold nanoparticles,[4,5] carbon nanomaterials,[6–8] transition-metal dichalcogenides,[9,10] and other organic polymers.[11,12] However, developing a reliable detection method to monitor the biodistribution and pharmacokinetics of these photothermal agents is still a challenge.[13,14] Though many theranostic platforms have been estabilished as the combining form of the therapeutic agents and imaging agents, the two agents may slowly dissociate from the carrier at different rates during the circulation in blood, leading to quite different biodistribution and pharmacokinetics.[15,16] Thus, it is important to find a photothermal agent which can serve as a contrast agent itself.

PAI is a powerful imaging technology based on optical excitation and ultrasound detection[19–21] Compared with the traditional optical imaging methodologies, PAI demonstrates many superiorities, such as low signal scattering in tissues, high resolution and sensitivity, rich optical contrasts, background- and speckle-free, which has been successfully used for in vivo imaging from organelles to organs.[22] The tumor site usually demonstrates photoacoustic singals, however, the intensity is rather low especially at early stage. Hence an effective PAI contrast agent is desirable. To guarantee a deep enough tissue penentration, the absorption window should tipically lie in the near infrared (NIR) region (700–900 nm). Considering that many photothermal agents also have strong absorption in the NIR region, it will be very convenient to combine PAI with PTT.[17,18] Many agents which have strong absorption in this optical window have been well investigated, among which carbon nanotubes are one of the most promising PAI contrast agents.[23] For example, Kim and his co-workers developed gold layer coated carbon nanotubes as photothermal and photoacoustic contrast agents for multimodal imaging.[24] Zerda and his collegues synthesized a family of enhanced PAI agents based on carbon nanotubes and optical dye molecules for ultra sensitive PAI.[25]

Apart from carbon nanotubes, many sp^2 carbonaceous nanomaterials may also serve as promising candidates for PAI and PTT. In that, single-walled carbon nanohorns (SWNHs) exhibit many advantages. Firstly, the size of SWNHs aggregate is 80–100 nm, which is optimal for the EPR effect and favors

D. Chen, S. Li, R. Li, M. Guan, Prof. C. Wang, Prof. C. Shu, Prof. L. Wan
Key Laboratory of Molecular Nanostructure and Nanotechnology
Institute of Chemistry
Chinese Academy of Sciences
and Beijing National Laboratory for Molecular Sciences
Beijing 100190, China
E-mail: shucy@iccas.ac.cn; wanlijun@iccas.ac.cn

C. Wang, Prof. Z. Liu
Jiangsu Key laboratory for Carbon-Based Functional Materials & Devices
Institute of Functional Nano & Soft Materials (FUNSOM)
Soochow University
Suzhou, Jiangsu 215123, China

X. Nie, Prof. C. Chen
CAS Key Laboratory for Biomedical Effects of Nanomaterials and Nanosafety National Center for Nanoscience and Technology (NCNST) No.11
1st North Street, Zhongguancun Beijing 100190, China

DOI: 10.1002/adfm.201401560

their accumulation in the tumor site when adminstrated with intraveneous injection.[26,27] Secondly, SWNHs are available in large quantities with high purity and free of metal catalysis, which avoids the introduction of toxic impurities during the synthetic process.[28,29] Thirdly, SWNHs are quite biocompatible and all kinds of toxicity evaluations have suggested there is no obviously acute toxicity both in vitro and in vivo.[30–33] To the best of our knowledge, the PAI guided PTT platform based on SWNHs has not yet been reported.[34–36] On the other hand, just like carbon nanotubes, SWNHs have a poor dispersibility in aqueous solution, which greatly limits their biomedical applicaiton. Though much attention has been focused on improving the dispersibility of SWNHs, developing water-dispersible SWNHs with long circulation in blood and high accumulation in targeting site remains to be a challenge.[37,38] Dai's group has reported a kind of PEG branched polymer, C_{18}PMH-PEG, for functionalization of nanomaterials, such as gold nanoparticles and SWNTs, which imparts the functionalized nanomaterials with excellent biocomptibility and ultra-long circulation time in blood.[39] As SWNHs share a lot in common with SWNTs, thus, the introduction of C_{18}PMH-PEG for functionalization of SWNHs may pave the way for the biomedical uses of SWNHs.

Herein, C_{18}PMH-PEG functionalized SWNHs (SWNHs/C_{18}PMH-PEG) was prepared for photoacoustic imaging guided photothermal therapy (**Figure 1**). The as-prepared SWNHs/C_{18}PMH-PEG possesses excellent stability and biocompatibility. As expected, it demonstrates significant heat generation under the irradiation of 808 nm laser. Moreover, it can also serve as a kind of promising PAI contrast agent. The tumor boundary can be clearly delineated after intravenous injection of SWNHs/C_{18}PMH-PEG. With the guidance of PAI, the optimal time for laser treatment is determined to be 24 h after intravenous injection, which guarantees a maximum accumulation of SWNHs/C_{18}PMH-PEG in the tumor site before the laser treatment for PTT. The photothermal ablation of tumor is realized without bringing any side effects. Thus, a theranostic platform based on SWNHs has been developed and is hopeful for biomedical uses in future.

2. Results and Discussions

2.1. Preparation and Characterization of SWNHs/C_{18}PMH-PEG

SWNHs were chacterized and FTIRspectrum, Raman spectrum, TEM image of prestine SWNHs were provided in the Supporting Information (SI, Figure S1–3). Stable SWNHs/C_{18}PMH-PEG aqueous solution was prepared simply by sonicating pristine SWNHs with C_{18}PMH-PEG for 1 h and the resulted solution was further purified by ultrafiltration (Scheme in SI). The obtained SWNHs/C_{18}PMH-PEG solution was highly stable in physiological medium such as water, phosphate buffer saline (PBS), cell culture medium and fetal bovine serum (FBS). Even centrifuged at 14 800 rpm for 1 h, no precipitation was observed at the bottom of the tubes. In contrast, the pristine SWNHs all precipitated under the same condition, leaving the supernatant almost transparent (**Figure 2**a). The obtained SWNHs/C_{18}PMH-PEG was characterized by dynamic light scattering (DLS) to demonstrate a hydrodynamic diameter of ≈120 nm. Considering the diameter of a single SWNHs aggregate is 80–100 nm, it is quite reasonable that the SWNHs aggregates are highly mono-dispersed after being modified with C_{18}PMH-PEG. Transmission electron microscopy (TEM) image of SWNHs/C_{18}PMH-PEG demonstrates that SWNHs/C_{18}PMH-PEG is mono-dispersed and the diameter is ≈80–100 nm, which is in accordance with the size of a single SWNHs aggregate (Figure 2c). When observed under a higher magnification, there is a blooming layer surrounding the SWNHs aggregate, suggesting the presence of C_{18}PMH-PEG

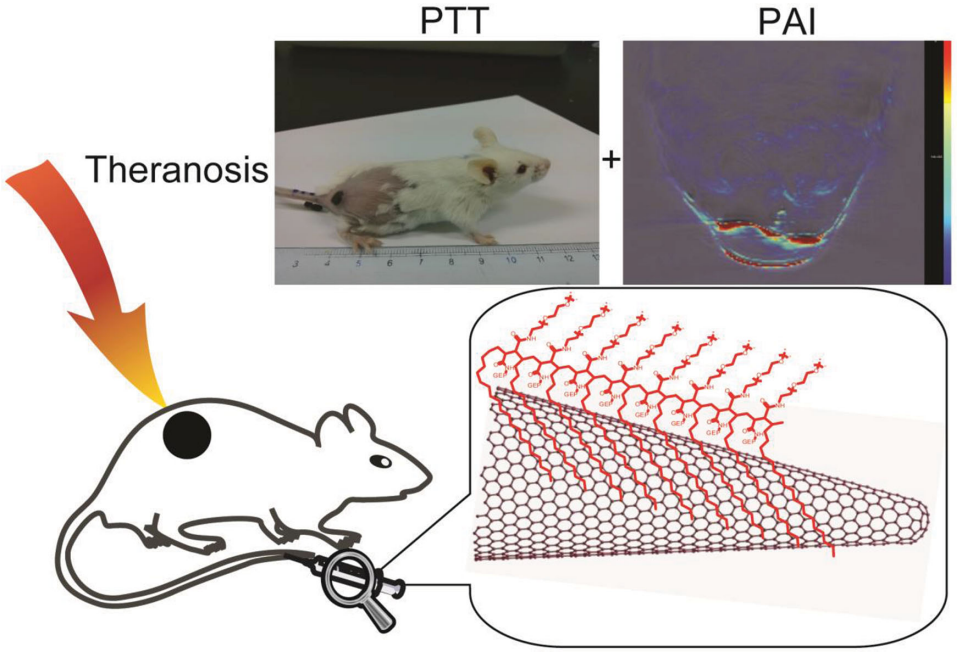

Figure 1. Scheme to illustrate the near-infrared photothermal therapy and photoacoustic imaging of SWNHs/C_{18}PMH-PEG.

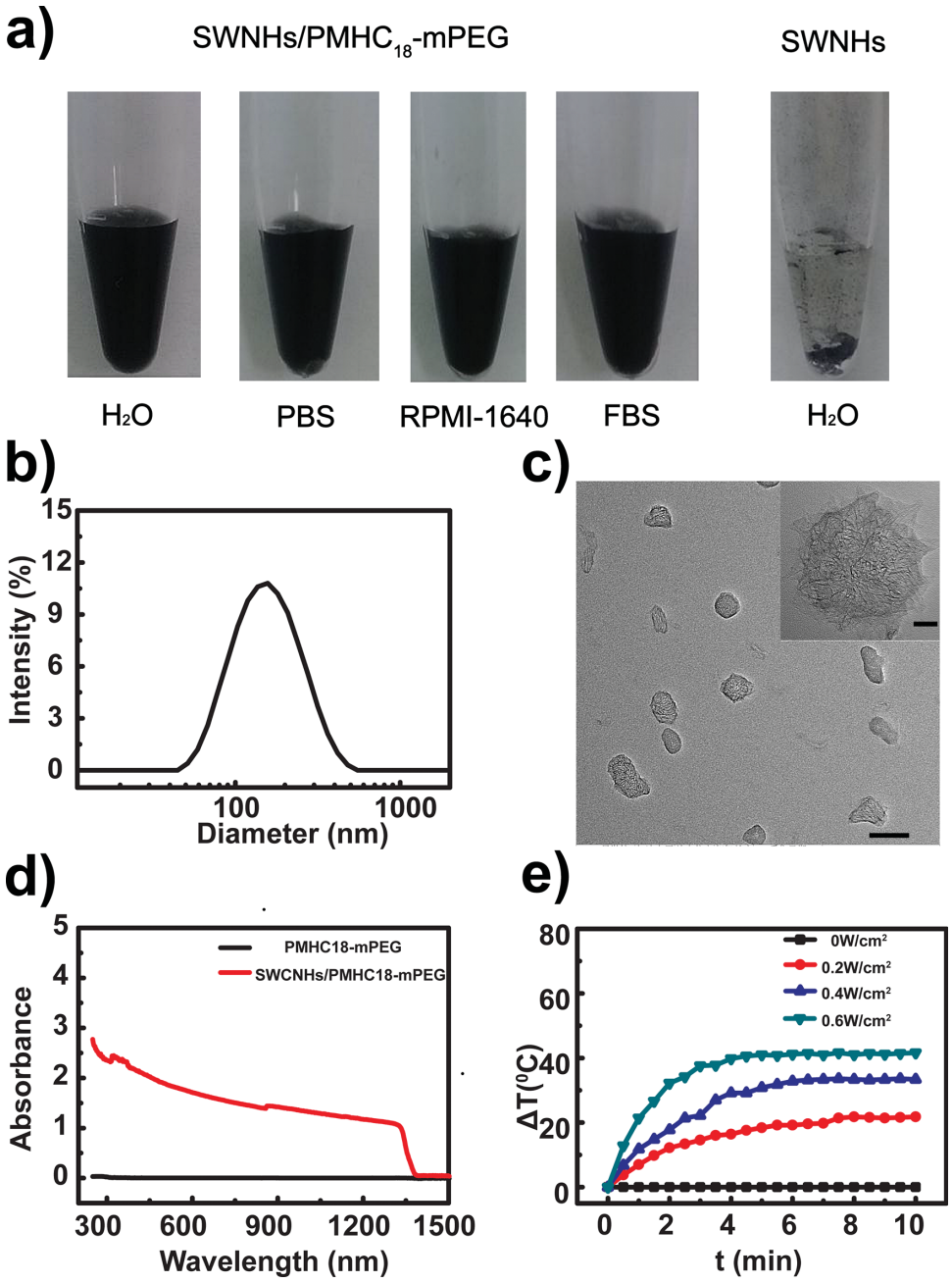

Figure 2. Characterization of SWNHs/C_{18}PMH-PEG. a) Photographs of SWNHs/C_{18}PMH-PEG in water, PBS, RPMI-1640 and FBS. b) Size distribution of SWNHs/C_{18}PMH-PEG measured by DLS. c) TEM image of SWNHs/C_{18}PMH-PEG, scale bar: 100 nm, Inset scale bar: 20 nm. d) UV/Vis/NIR absorption of SWNHs/C_{18}PMH-PEG and C_{18}PMH-PEG in aqueous solution. e) Temperature elevation curves of SWNHs/C_{18}PMH-PEG aqueous solution (SWNHs concentration, 0.1 mg mL^{-1}) exposed to a series of laser power densities (0, 0.2, 0.4, 0.6 W cm^{-2}).

(Inset of Figure 2c). It is speculated that the hydrophobic alkyl chains are anchored onto the surface of SWNHs and the hydrophilic PEG chains extend to the aqueous solution, which endows SWNHs/C_{18}PMH-PEG with high stability in all kinds of aqueous medium. The UV/Vis/NIR absorption spectra show that SWNHs/C_{18}PMH-PEG possesses strong absorption at the range of 300–1300 nm (Figure 2d). However, C_{18}PMH-PEG alone doesn't demonstrate obvious absorption, indicating that the characteristic absorbance largely originates from SWNHs. The photothermal property of SWNHs/C_{18}PMH-PEG was also evaluated. The result reveals that SWNHs/C_{18}PMH-PEG possesses rather high photothermal conversion efficiency. The temperature elevation of the SWNHs/C_{18}PMH-PEG solution (SWNHs concentration, 0.1 mg mL^{-1}) could reach as high as 41 °C within 5 min under an 808 nm laser irradiation with a power density of 0.6 W cm^{-2} and then maintains at this temperature as a result of heat exchange with the environment (Figure 2e). Notably, this temperature elevation is strongly

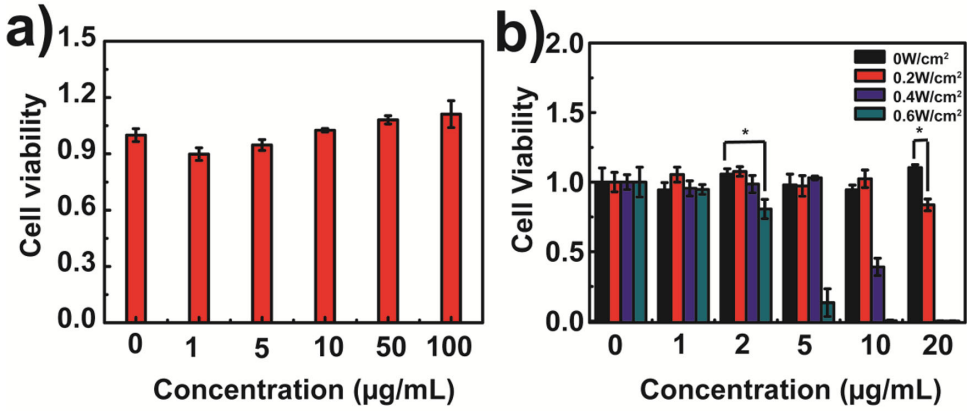

Figure 3. In vitro cell viability. 4T1 cells incubated with SWNHs/C_{18}PMH-PEG in different concentrations a) without and b) with the 808 nm laser irradiation at different power densities.

concentration- and laser power density-dependent (Figure S5 and S6, SI). Thus, the temperature elevation could be under fine control simply by adjusting the concentration of SWNHs/C_{18}PMH-PEG and the laser power density, which facilitates the application of SWNHs/C_{18}PMH-PEG as a photothermal agent for cancer cell killing and tumor ablation there-in-after.

2.2. Cell Growth Inhibition Assays

Figure 3a,b demonstrate the cell growth inhibition of 4T1 cells incubated with SWNHs/C_{18}PMH-PEG either with or without an 808 nm laser irradiation. For non-irradiated 4T1 cells, SWNHs/C_{18}PMH-PEG doesn't show any significant cell growth inhibition at concentrations ranging from 1 to 100 μg mL^{-1}, indicating that SWNHs/C_{18}PMH-PEG is of excellent biocompatibility. However, the cell viability decreases dramatically when exposed to the 808 nm laser irradiation. The growth inhibition of 4T1 cells is strongly dependent on the concentration of SWNHs/C_{18}PMH-PEG and the power density of 808 nm laser. When the 4T1 cells were incubated with merely 2 μg mL^{-1} SWNHs/C_{18}PMH-PEG, only those exposed to 808 nm laser with power density of 0.6 W cm^{-2} could lead to significant inhibition to 4T1 cells. However, if the concentration of incubated SWNHs/C_{18}PMH-PEG increases to 20 μg mL^{-1}, those with the irradiation of 0.2 W cm^{-2} laser can result in obvious damage to 4T1 cells. This again demonstrates that the photothermal heating of SWNHs/C_{18}PMH-PEG is concentration- and laser power density- dependent, which is closely related with the growth inhibition of 4T1 cells.

2.3. Photoacoustic Imaging of Mice

Due to the strong absorption in the NIR region, SWNHs/C_{18}PMH-PEG can not only be employed as good photothermal agents, but also prove to be an excellent photoacoustic imaging agent. **Figure 4**a shows the photoacoustic images of 4T1 tumor bearing mice i.v. injected with SWNHs/C_{18}PMH-PEG (2 mg mL^{-1}, 200 μL). The photoacoustic image of tumor and the surrounding tissues were recorded at different time points (1, 4, 24, 48 h). The result reveals that SWNHs/C_{18}PMH-PEG is an excellent photoacoustic imaging agent, which can significantly illuminate the tumor site and contribute to delineate the margins of the tumour clearly. The photoacoustic signals of SWNHs/C_{18}PMH-PEG at the tumor site continue to increase in 24 h after i.v. injection, demonstrating an continuing accumulation of SWNHs/C_{18}PMH-PEG at the tumor site. It has been reported that the SWNTs/C_{18}PMH-PEG could accumulate at the tumor site through the EPR effect.[8,40] Considering the unique morphology and size of SWNHs/C_{18}PMH-PEG that favors the passive targeting of the tumor site through the EPR effect,[41] it is quite reasonable to ascribe this accumulation of SWNHs/C_{18}PMH-PEG at the tumor site to the EPR effect.

We also calculated the mean signal intensity and maximum mean signal intensity of the region of interest (ROI) (Figure 4b). The signal intensity increases with the time after injection and reaches the maximum at ≈24 h post-injection, indicating a continuing accumulation of SWNHs/C_{18}PMH-PEG at the tumor site via blood circulation. Compared with the photoacoustic signal of the tumor site itself, the accumulation of SWNHs/C_{18}PMH-PEG could increase the signal by five times, which garantees a high signal to noise ratio for the tumor imaging. The signal intensity showes a slightly decrease at 48 h post-injection, but still, much stronger than that at 4 h post injection, suggesting an ultra long blood circulation of SWNHs/C_{18}PMH-PEG. Therefore, 24 h after i.v. injection of SWNHs/C_{18}PMH-PEG is determined to be the optimal time for the 808 nm irradiation, which could guarantee a maximum accumulation of SWNHs/C_{18}PMH-PEG at the tumor site and the best PTT efficacy. In a word, the photoacoustic imaging of SWNHs/C_{18}PMH-PEG is successfully employed as an effective method to guide the subsequent photothemal ablation of the tumor.

Intriguingly, the central part of the tumor is hardly illuminated as the photoacoustic signal of SWNHs/C_{18}PMH-PEG could hardly be detected. This is quite different from the previously reported results of SWNTs and nanographenes, in which the central part of the tumor rather than its boundary could be clearly visualized.[23,42,43] It has been reported that the penetration of tumors for nanoparticles is closely related to the size and shape.[44,45] It is speculated that SWNHs/C_{18}PMH-PEG is inclined to sustain in the tumor vessels rather than to penetrate

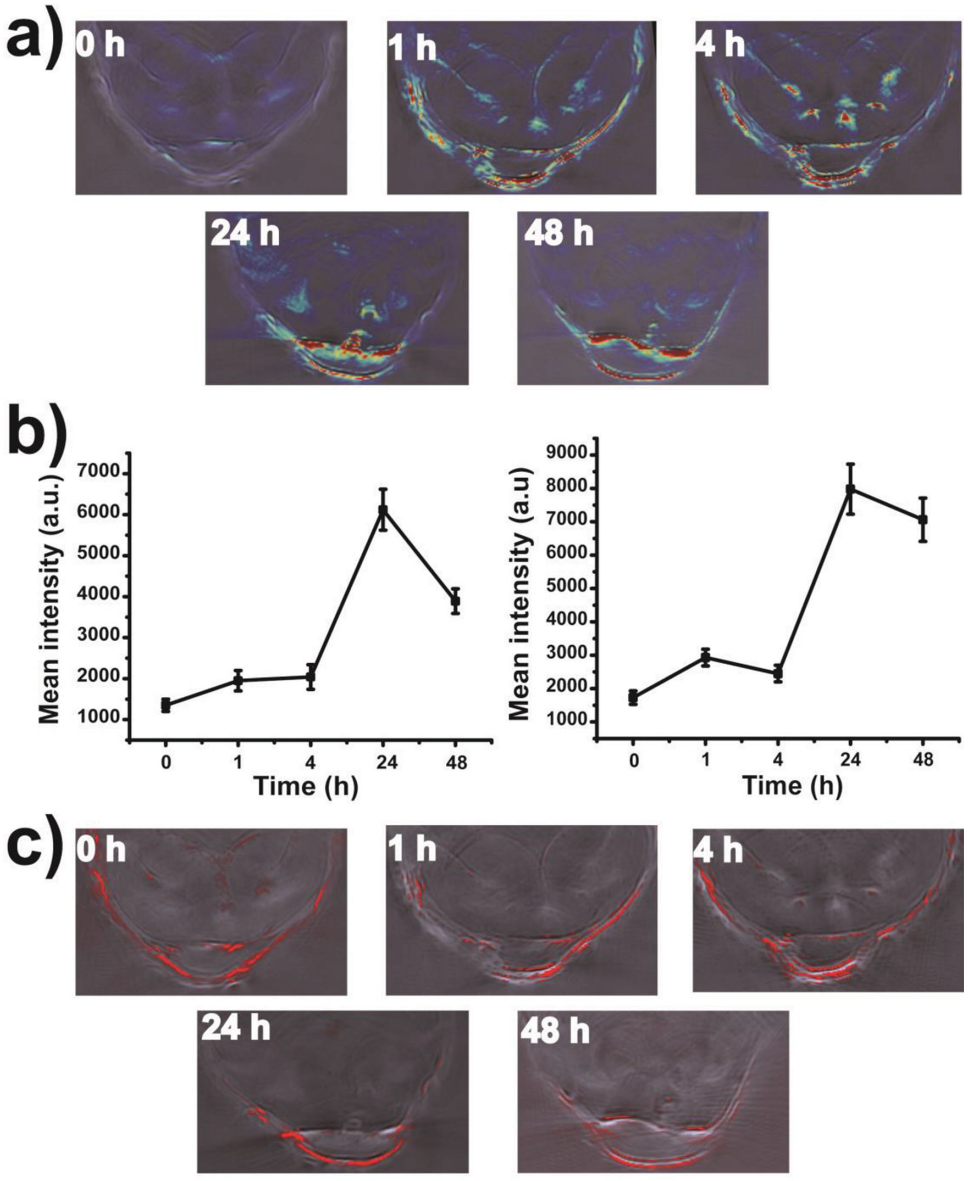

Figure 4. Time-dependent in vivo PAI of tumor bearing mice after intravenously injected with SWNHs/C_{18}PMH-PEG. a) Photoacoustic images of tumor in mice after intravenous injection with SWNHs/C_{18}PMH-PEG for 1 h, 4 h, 24 h, 48 h. b) Mean signal intensity and maximum mean signal intensity of region of intrest (ROI) at different time after i.v. injeciton. c) Photoacoustic images of hemoglobin in tumor at different time after i.v. injection.

deep in tumor as their counterparts, SWNTs and nano graphenes. The imaging of hemoglobin verifies our hypothesis (Figure 4c) since there is a high conincidence of the photoacoustic signals of hemoglobin and SWNHs/C_{18}PMH-PEG. That is to say, the SWNHs/C_{18}PMH-PEG imaged by PAI is located the blood vessels as hemoglobin does.

2.4. Phototherapy

Before the implementation of photothermal ablation of tumor in mice, an optimal laser power density was determined. 4T1 tumor bearing female Balb/c mice were i.v. injected with SWNHs/C_{18}PMH-PEG (2 mg mL^{-1}, 200 μL). Under the guidance of the PAI results, the laser treatment was conducted 24 h after i.v. injection to gurantee a maximum accumulation of SWNHs/C_{18}PMH-PEG at the tumor site. Then the temperature elevation of tumor exposed to laser irradiation with different power density was monitored (Fiugre S7, SI). It was found that the temperature of the tumor could reach ≈55 °C when exposed to 0.4 W cm^{-2} laser irradiation. It has been reported that this temperature elevation is high enough for tumor ablation,[43] hence the optimal laser power density was set as 0.4 W cm^{-2}. The phototherapy of tumor bearing mice was conducted as the experimental section mentioned and the tumor size and weight of the mice were monitored during the experiment. **Figure 5**b demonstrates the relative tumor size curves of the four groups. It is found that only the mice injected with SWNHs/C_{18}PMH-PEG

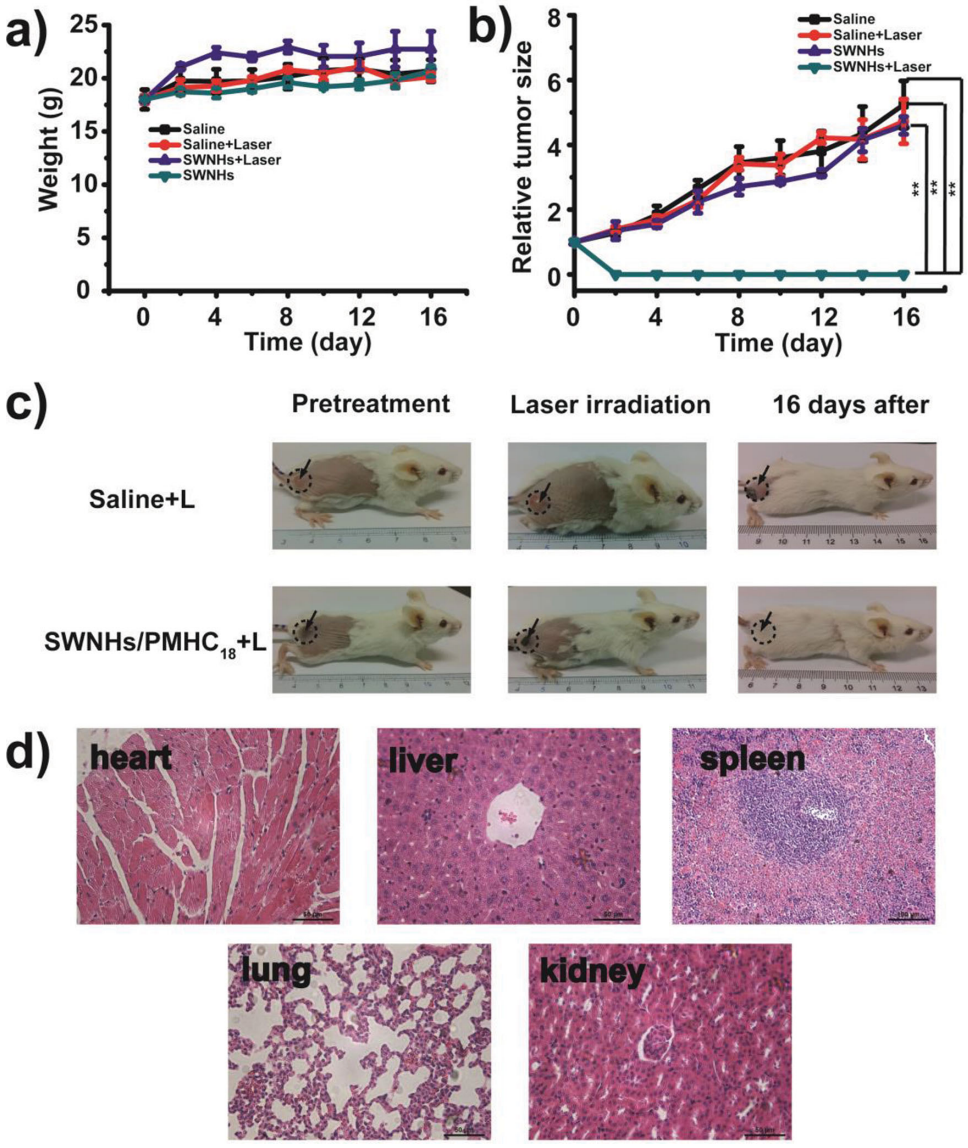

Figure 5. In vivo photothermal therapy. a) The body weight change of the mice after treatment. b) The tumor growth curves of the mice after treatment. c) Representative photographs of 4T1 tumor bearing mice i.v. injected with either saline or SWNHs/C_{18}PMH-PEG and exposed to laser treatment. d) H&E staining slice of heart, liver, spleen, lung and kidney in mice after PTT.

and subsequently treated with the laser show tumor ablation by PTT, and the tumors in the other three groups continue growing during the observation. We also monitored the body weight of the mice to roughly evaluate the toxicity of SWNHs/C_{18}PMH-PEG. The mice injected with SWNHs/C_{18}PMH-PEG don't suffer significant body weight loss during the experiment, suggesting that there is no obvious acute toxicity (Figure 5a). Figure 5c shows the photographs of the mice in the laser treated groups. The tumors of the mice injected with SWNHs/C_{18}PMH-PEG become dark 24 h post-injection, indicating an obvious accumulation in the tumor site, which is highly coincident with the PAI results. After the laser treatment, the ablation of tumors was observed, leaving the tumor site a black scar. The crusts fell off one week later and the hairs began to grow without a recurrence of the tumor, which suggests a complete tumor ablation by PTT. In contrast, the tumor size of mice injected with saline and then exposed to laser irradiation don't show any difference in comparison with the control groups, suggesting that the laser alone could not affect the development of 4T1 tumors. The toxicity of SWNHs/C_{18}PMH-PEG was further evaluated by analyzing the tissue slices of the mice administrated with SWNHs/C_{18}PMH-PEG. No obvious inflammation, cell necrosis and apoptosis are observed in heart, liver, spleen, lung and kidney, indicating there is no obvious side effect (Figure 5d).

3. Conclusion

In summary, we developed a theranostic platform using highly stable and biocompatible SWNHs/C_{18}PMH-PEG for

PAI guided phototherapy. The strong absorption in the NIR region and excellent photothermal property make SWNHs/C_{18}PMH-PEG a promising candidate for PAI and PTT simultaneously. The experimental results demonstrate that the photothermal-induced death of cancer cells is SWNHs/C_{18}PMH-PEG concentration- and laser power density-dependent. The in vivo experimental results further reveal that the margins of tumor can be clearly delineated as a result of accumlation of SWNHs/C_{18}PMH-PEG in the tumor vessels as PAI proved. The PAI result also indicates that the accumulation of SWNHs/C_{18}PMH-PEG reaches the maximum 24 h after i.v. injection, which provides a guideline for the subsequent PTT. The PTT results show an effective tumor ablation and no recurrence is observed during the experiment. The body weight monitoring and tissue slices evaluation suggest that there is no obvious side effect in the mice injected with SWNHs/C_{18}PMH-PEG. Hence, a safe and effective theranostic agent based on SWNHs is proposed and hopefully extended to medical uses.

4. Experimental Section

Materials: 1-ethyl-3-(3-dimethylaminopropyl)-carbodiimide hydrochloride (EDC) was obtained from Shanghai RichJoint Chemical Reagents Co. Ltd, China. dichloromethane and triethylamine were purchased from Sinopharm Chemical Reagent Co. Ltd., China. Poly(maleic anhydride-alt-1-octadecene) (C_{18}PMH) were purchased from Sigma Company. Ltd. Cell Counting Kit-8 (CCK-8) was purchased from Dojindo Laboratories (Japan). mPEG-NH_2 (5 k) was obtained from PegBio (Suzhou, China). All commercially available solvents and reagents were analytical grade and were used without further purification.

Synthesis of C_{18}PMH-PEG: C_{18}PMH-PEG was synthesized according to the previously reported.[39] Briefly, 10 mg of C_{18}PMH and 143 mg of mPEG-NH_2 (5 kDa) were pre-dissolved in 5 mL of dichloromethane and 6 mL of triethylamine before 11 mg EDC was added. After stirring for 24 h, the product was transferred to a dialysis bag (MWCO, 14 kDa) and dialyzed against distilled water for 2 days to remove the unreacted mPEG-NH_2. The final product was obtained after lyophilization and was stored at –20 °C for future use.

Synthesis of SWNHs/C_{18}PMH-PEG: 1 mg SWNHs were sonicated in 5 mL of water with 10 mg C_{18}PMH-PEG for 1 h. The excess of C_{18}PMH-PEG was removed by filtration through a 0.2 μm polycarbonate membrane for several times.

Characterization of SWNHs/C_{18}PMH-PEG: The size of SWNHs/C_{18}PMH-PEG was characterized by dynamic light scattering (Malvern Zetasizer Nano ZS 90) at 25 °C. Transmission electron microscope (TEM) image was obtained from JEM-2011 (JEOL, Japan) operated at 200 kV. NIR absorption spectrum was recorded with PE Lambda 750 UV/Vis/NIR spectrophotometer.

Temperature Elevation Assay Induced by Laser Irradiation: SWNHs/C_{18}PMH-PEG (SWNHs concentration, 100 μg mL^{-1}) in PBS (500 μL) was irradiated with 808 nm laser light with a power density of 0, 0.2, 0.4, 0.6 W cm^{-2} for 10 min, respectively. The temperature of the solutions was recorded by an infrared thermometer mini hand-held laser infrared temperature measurement Gun (Fluke F59, USA).

Cell Culture: 4T1 cells were cultured in Roswell Park Memorial Institute-1640 (RPMI-1640) cell culture medium, supplemented with 10% fetal bovine serum (FBS) and 1% penicillin/Streptomycin (PS) at 37 °C under a humidified atmosphere with 5% CO_2.

Photothermal Treatment and Cell Growth Inhibition Assays: Cell viabilities of 4T1 cells incubated with SWNHs/C_{18}PMH-PEG solution either with or without 808 nm-laser treatment were determined by CCK-8 assays, respectively. First, 4T1 cells with ≈5 × 10^4 cells per milliliter density were seeded into a 96-well culture plate with 200 μL of RPMI-1640 supplemented with 10% FBS and 1% PS in each well, and incubated at 37 °C under a humidified atmosphere with 5% CO_2 for 24 h. Then the aged culture medium was replaced by freshly prepared culture medium containing either SWNHs/C_{18}PMH-PEG solution in a series of gradient concentrations (SWNHs concentration, 0, 1, 2, 5, 10, 20 μg mL^{-1}). For the 808 nm laser treatment groups, the 96-well culture plate was immediately irradiated by the 808 nm laser at a series of power densities (0, 0.2, 0.4, 0.6 W cm^{-2}) for 10 min only once. After that, the culture medium was replaced by fresh RPMI-1640 and incubated for another 24 h. Then the culture medium was removed and 100 μL of DMEM without phenol red and 10 μL of CCK-8 were added into each well. After incubated for another 1 h, the absorbance of each well was measured at 450 nm by a microplate reader.

Animal Experiment: 5-week-old female Balb/c mice were purchased from Nanjing Peng Sheng Biological Technology Co. Ltd and all animal experiments were conducted under protocols approved by Soochow University Laboratory Animal Center. 40 μL of ≈5 × 10^5 4T1 cells μL^{-1} suspension was subcutaneously injected into the right flank of each mouse.

Photoacoustic Imaging: Mice bearing 4T1 tumors were administrated with SWNHs/C_{18}PMH-PEG (SWNHs concentration, 2 mg mL^{-1}, 200 μL) through tail vein injection. Photoacoustic imaging was performed by an ultra-high resolution small animal imaging system (MOST invison 128, iThera) at different intervals (0 h, 1 h, 4 h, 24 h, 48 h).

Photothermal Therapy: 24 tumor-bearing Balb/c mice were randomly distributed into 4 groups, with 6 mice per group. Mice bearing 4T1 tumors in the experiment group were tail vein injected with 200 μL of SWNHs/C_{18}PMH-PEG (SWNHs concentration, 2 mg mL^{-1}) solution. For control groups, mice were treated with the same volume of saline. The laser-treated groups were irradiated with an 808 nm NIR laser (Hi-Tech Optoelectronics Co., Ltd. Beijing, China) at a power density of 0.4 W cm^{-2} for 10 min only once. The tumor sizes were measured with an electronic digital caliper every other day and calculated as the volume = $a \times b^2/2$, a and b referred to the length and width of the tumor, respectively. Relative tumor volumes were obtained by dividing the initial tumor size before laser treating.

Tumor Sections for Histological Examination: For histological examination, tumor tissues in the center of tumors were fixed in 4% formalin and conducted with paraffin embedded sections for H&E staining. The slices were examined by a digital microscope (Leica QWin).

Statistical Analysis: The statistical analysis of the samples was conducted by Student's t-test, $p < 0.05$ were considered statistically significant (*) and $p < 0.01$ were very significant (**). All data reported are means ± standard deviations, unless otherwise noted.

Supporting Information

Supporting Information is available from the Wiley Online Library or from the author.

Acknowledgements

This work was supported by the National Natural Science Foundation of China (Grant Nos. 21121063, 21127901, 31170963) and the Chinese Academy of Sciences. The authors thank Sumio Iijima and Masako Yudasaka (NEC) for kindly providing SWNHs.

Received: May 14, 2014
Revised: July 6, 2014
Published online: August 26, 2014

[1] J. F. Lovell, C. S. Jin, E. Huynh, H. Jin, C. Kim, J. L. Rubinstein, W. C. Chan, W. Cao, L. V. Wang, G. Zheng, *Nat. Mater.* **2011**, *10*, 324.
[2] X. Huang, I. H. El-Sayed, W. Qian, M. A. El-Sayed, *J. Am. Chem. Soc.* **2006**, *128*, 2115.
[3] S. Wang, P. Huang, L. Nie, R. Xing, D. Liu, Z. Wang, J. Lin, S. Chen, G. Niu, G. Lu, *Adv. Mater.* **2013**, *25*, 3055.
[4] X. Wang, C. Wang, L. Cheng, S. T. Lee, Z. Liu, *J. Am. Chem. Soc.* **2012**, *134*, 7414.
[5] H. Liu, T. Liu, X. Wu, L. Li, L. Tan, D. Chen, F. Tang, *Adv. Mater.* **2012**, *24*, 755.
[6] K. Yang, S. Zhang, G. Zhang, X. Sun, S. T. Lee, Z. Liu, *Nano Lett.* **2010**, *10*, 3318.
[7] J. R. Whitney, S. Sarkar, J. Zhang, T. Do, T. Young, M. K. Manson, T. A. Campbell, A. A. Puretzky, C. M. Rouleau, K. L. More, D. B. Geohegan, C. G. Rylander, H. C. Dorn, M. N. Rylander, *Lasers Surg. Med.* **2011**, *43*, 43.
[8] J. T. Robinson, K. Welsher, S. M. Tabakman, S. P. Sherlock, H. Wang, R. Luong, H. Dai, *Nano Res.* **2010**, *3*, 779.
[9] L. Cheng, J. Liu, X. Gu, H. Gong, X. Shi, T. Liu, C. Wang, X. Wang, G. Liu, H. Xing, *Adv. Mater.* **2014**, *26*, 1794.
[10] S. S. Chou, B. Kaehr, J. Kim, B. M. Foley, M. De, P. E. Hopkins, J. Huang, C. J. Brinker, V. P. Dravid, *Angew. Chem. Int. Ed.* **2013**, *125*, 4254.
[11] Y. Liu, K. Ai, J. Liu, M. Deng, Y. He, L. Lu, *Adv. Mater.* **2013**, *25*, 1353.
[12] L. Cheng, K. Yang, Q. Chen, Z. Liu, *ACS Nano* **2012**, *6*, 5605.
[13] M. Zhang, Y. Tahara, M. Yang, X. Zhou, S. Iijima, M. Yudasaka, *Adv. Healthcare Mater.* **2013**, *3*, 239.
[14] Z. Liu, C. Davis, W. Cai, L. He, X. Chen, H. Dai, *Proc. Natl. Acad. Sci.* **2008**, *105*, 1410.
[15] J. Xie, S. Lee, X. Chen, *Adv. Drug Delivery Rev.* **2010**, *62*, 1064.
[16] J. U. Menon, P. Jadeja, P. Tambe, K. Vu, B. Yuan, K. T. Nguyen, *Theranostics* **2013**, *3*, 152.
[17] P. Huang, J. Lin, W. Li, P. Rong, Z. Wang, S. Wang, X. Wang, X. Sun, M. Aronova, G. Niu, *Angew. Chem. Int. Ed.* **2013**, *125*, 14208.
[18] W. Lu, Q. Huang, G. Ku, X. Wen, M. Zhou, D. Guzatov, P. Brecht, R. Su, A. Oraevsky, L. V. Wang, *Biomaterials* **2010**, *31*, 2617.
[19] Y. Wang, X. Xie, X. Wang, G. Ku, K. L. Gill, D. P. O'Neal, G. Stoica, L. V. Wang, *Nano Lett.* **2004**, *4*, 1689.
[20] L. V. Wang, S. Hu, *Science* **2012**, *335*, 1458.
[21] M. Xu, L. V. Wang, *Rev. Sci. Instrum.* **2006**, *77*, 041101.
[22] G. Ku, L. V. Wang, *Opt. Lett.* **2005**, *30*, 507.
[23] A. De La Zerda, C. Zavaleta, S. Keren, S. Vaithilingam, S. Bodapati, Z. Liu, J. Levi, B. R. Smith, T.-J. Ma, O. Oralkan, *Nat. Nanotechnol.* **2008**, *3*, 557.
[24] J.-W. Kim, E. I. Galanzha, E. V. Shashkov, H.-M. Moon, V. P. Zharov, *Nat. Nanotechnol.* **2009**, *4*, 688.
[25] A. de la Zerda, S. Bodapati, R. Teed, S. N. Y. May, S. M. Tabakman, Z. Liu, B. T. Khuri-Yakub, X. Chen, H. Dai, S. S. Gambhir, *ACS Nano* **2012**, *6*, 4694.
[26] S. Iijima, M. Yudasaka, R. Yamada, S. Bandow, K. Suenaga, F. Kokai, K. Takahashi, *Chem. Phys. Lett.* **1999**, *309*, 165.
[27] S. Bandow, F. Kokai, K. Takahashi, M. Yudasaka, L. Qin, S. Iijima, *Chem. Phys. Lett.* **2000**, *321*, 514.
[28] T. Saito, S. Ohshima, W.-C. Xu, H. Ago, M. Yumura, S. Iijima, *J. Phys. Chem. B* **2005**, *109*, 10647.
[29] D. N. Futaba, K. Hata, T. Yamada, K. Mizuno, M. Yumura, S. Iijima, *Phys. Rev. Lett.* **2005**, *95*, 056104.
[30] T. Murakami, M. Nakatani, M. Kokubo, H. Nakatsuji, M. Inada, H. Imahori, M. Yudasaka, S. Iijima, K. Tsuchida, *Nanosci. Nanotechnol. Lett.* **2013**, *5*, 402.
[31] J. Miyawaki, M. Yudasaka, T. Azami, Y. Kubo, S. Iijima, *ACS Nano* **2008**, *2*, 213.
[32] Y. Tahara, J. Miyawaki, M. Zhang, M. Yang, I. Waga, S. Iijima, H. Irie, M. Yudasaka, *Nanotechnology* **2011**, *22*, 265106.
[33] J. Guerra, M. A. Herrero, B. Carrión, F. C. Pérez-Martínez, M. Lucío, N. Rubio, M. Meneghetti, M. Prato, V. Ceña, E. Vázquez, *Carbon* **2012**, *50*, 2832.
[34] E. Miyako, T. Deguchi, Y. Nakajima, M. Yudasaka, Y. Hagihara, M. Horie, M. Shichiri, Y. Higuchi, F. Yamashita, M. Hashida, *Proc. Natl. Acad. Sci.* **2012**, *109*, 7523.
[35] M. Zhang, T. Murakami, K. Ajima, K. Tsuchida, A. S. Sandanayaka, O. Ito, S. Iijima, M. Yudasaka, *Proc. Natl. Acad. Sci.* **2008**, *105*, 14773.
[36] F. Zhou, S. Wu, Y. Yuan, W. R. Chen, D. Xing, *Small* **2012**, *8*, 1543.
[37] T. Murakami, J. Fan, M. Yudasaka, S. Iijima, K. Shiba, *Mol. Pharm.* **2006**, *3*, 407.
[38] S. Matsumura, S. Sato, M. Yudasaka, A. Tomida, T. Tsuruo, S. Iijima, K. Shiba, *Mol. Pharm.* **2009**, *6*, 441.
[39] G. Prencipe, S. M. Tabakman, K. Welsher, Z. Liu, A. P. Goodwin, L. Zhang, J. Henry, H. Dai, *J. Am. Chem. Soc.* **2009**, *131*, 4783.
[40] Z. Liu, K. Chen, C. Davis, S. Sherlock, Q. Cao, X. Chen, H. Dai, *Cancer Res.* **2008**, *68*, 6652.
[41] A. Albanese, P. S. Tang, W. C. Chan, *Annu. Rev. Biomed. Eng.* **2012**, *14*, 1.
[42] A. D. L. Zerda, Z. Liu, S. Bodapati, R. Teed, S. Vaithilingam, B. T. Khuri-Yakub, X. Chen, H. Dai, S. S. Gambhir, *Nano Lett.* **2010**, *10*, 2168.
[43] K. Yang, L. Hu, X. Ma, S. Ye, L. Cheng, X. Shi, C. Li, Y. Li, Z. Liu, *Adv. Mater.* **2012**, *24*, 1868.
[44] V. P. Chauhan, R. K. Jain, *Nat. Mater.* **2013**, *12*, 958.
[45] R. K. Jain, *J. Clin. Oncol.* **2013**, *31*, 2205.